JOC*Article*

Cu(II)-Mediated Generation of Triarylamine Radical Cations and Their Dimerization. An Easy Route to Tetraarylbenzidines

Kesavapillai Sreenath, Chettiyam Veettil Suneesh, Venugopal K. Ratheesh Kumar, and Karical R. Gopidas*

Photosciences and Photonics, Chemical Sciences and Technology Division, National Institute for Interdisciplinary Science and Technology, Trivandrum 695 019, India

gopidaskr@rediffmail.com

Received February 12, 2008

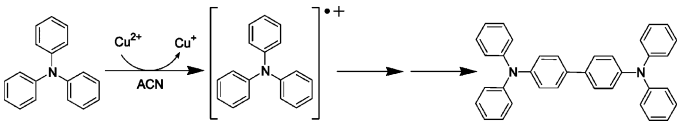

Triphenylamine (TPA) derivatives react with Cu^{2+} in acetonitrile to give TPA radical cations which undergo dimerization and deprotonation reactions to yield tetraphenylbenzidines (TPB). Synthetic utility of this reaction is demonstrated using several triphenylamine derivatives, and yields in excess of 80% are obtained in most cases. Involvement of the amine radical cations in these reactions was confirmed by ESR and absorption spectroscopic studies. A mechanism consistent with all observations is proposed. This study also revealed a very good correlation between the free energy change for radical cation formation and product yields.

Introduction

Tetraphenylbenzidine (TPB) and its derivatives have received considerable attention because of their applications as photoconductors and hole-transporting layers in organic light-emitting diodes, organic solar cells, organic field effect transistors, and xerography.[1−7] In each of these applications, materials of electronic grade purity are required for optimal device performance. At present, TPB derivatives are most generally prepared by the Ullmann condensation reaction between diphenylamine and an unactivated aryl halide in the presence of a copper catalyst (metal, alloy, or salt) as shown in Scheme 1.

High temperatures and extended reaction times are often required, and the yields are generally unpredictable because of side reactions such as dehalogenation and homocoupling. Several attempts were made to moderate the Ullmann reaction conditions. For example, Goodbrand et al.[8a] and Lu et al.[8b] employed 1,10-phenanthroline ligand along with cuprous chloride and KOH in aromatic hydrocarbon solvents (toluene or xylene) at refluxing temperatures to obtain good yields of TPB

SCHEME 1. Ullmann Synthesis of TPB Derivatives

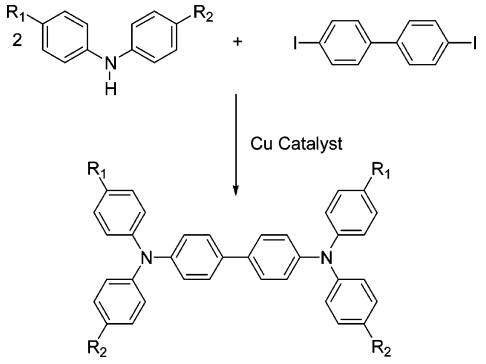

* To whom correspondence should be addressed. Fax: 91-471-2490186.

(1) (a) Thelakkat, M. *Macromol. Mater. Eng.* **2002**, *287*, 442. (b) Thelakkat, M.; Fink, R.; Haubner, F.; Schmidt, H.-W. *Macromol. Symp.* **1997**, *125*, 157.

(2) Adachi, C.; Tokito, S.; Tsutsui, T.; Saito, S. *Jpn. J. Appl. Phys.* **1988**, *27*, L269.

(3) Adachi, C.; Nagai, K.; Tamoto, N. *Appl. Phys. Lett.* **1995**, *66*, 2679.

(4) Handa, S.; Wietasch, H.; Thelakkat, M.; Durrant, J. R.; Haque, S. A. *Chem. Commun.* **2007**, *17*, 1725.

(5) Yang, Y.; Xue, S.; Liu, S.; Huang, J.; Shen, J. *Appl. Phys. Lett.* **1996**, *69*, 377.

(6) Saragi, T. P. I.; Fuhrmann-Lieker, T.; Salbeck, J. *Adv. Funct. Mater.* **2006**, *16*, 966.

(7) Theys, R. D.; Sosnovsky, G. *Chem. Rev.* **1997**, *97*, 83.

(8) (a) Goodbrand, H. B.; Hu, N.-X. *J. Org. Chem.* **1999**, *64*, 670. (b) Lu, J.; Hlil, A. R.; Sun, Y.; Hay, A. S.; Maindron, T.; Dodelet, J.-P.; D'Iorio, M. *Chem. Mater.* **1999**, *11*, 2501. (c) Liu, Y.-H.; Chen, C.; Yang, L.-M. *Tetrahedron Lett.* **2006**, *47*, 9275. (d) Low, P. J.; Paterson, M. A. J.; Goeta, A. E.; Yufit, D. S.; Howard, J. A. K.; Cherryman, J. C.; Tackley, D. R.; Brown, B. *J. Mater. Chem.* **2004**, *14*, 2516. (e) Low, P. J.; Paterson, M. A. J.; Yufit, D. S.; Howard, J. A. K.; Cherryman, J. C.; Tackley, D. R.; Brook, R.; Brown, B. *J. Mater. Chem.* **2005**, *15*, 2304. (f) Wang, X.; Chen, Z.; Ogino, K.; Sato, H.; Strzelec, K.; Miyata, S.; Luo, Y.; Tan, H. *Macromol. Chem. Phys.* **2002**, *203*, 739.

10.1021/jo800349n CCC: $40.75
Published on Web 03/22/2008

derivatives. Ligands such as 1,4-diazabuta-1,3-diene,[8c] 18-crown-6,[8d,e] or tri-*tert*-butylphosphine[8f] along with Cu salts and a base (K_2CO_3 or *t*-BuOK) were employed by others. All these modifications could not eliminate the requirements of high reaction temperatures (125−150 °C) and long reaction times (3−45 h). Palladium-catalyzed aromatic amination reactions developed by Buchwald and Hartwig appear promising, but these have not been applied for the synthesis of TPB derivatives.[9] In this context, new synthetic methodologies, which involve mild reaction conditions and cheap chemicals, are very desirable. Herein we report a simple and highly efficient method, which involves the dimerization of triarylamine radical cations, for the synthesis of TPB and several of its derivatives. It is to be mentioned here that dimerization of electrochemically generated triphenylamine radical cations to TPB derivatives were studied previously by several groups,[10] but the electrochemical method has not yet evolved as synthetically useful for the preparation of TPB derivatives.

Results and Discussion

Recently, we have introduced a very simple and effective method for the generation of aromatic amine radical cations.[11] The reaction involved mixing of the aromatic amines with 1 equiv of $Cu(ClO_4)_2$ in acetonitrile (ACN) solution. The amine radical cation is generated as a result of single electron transfer from the amine to Cu^{2+} as in eq 1.

$$\text{amine} + Cu^{2+} \rightarrow \text{amine}^{\bullet+} + Cu^{+} \qquad (1)$$

We have shown that a large number of aromatic amines undergo this reaction. Taking *N*,*N*-dialkylanilines as examples, we have recently shown that this method can be effectively explored for generating the amine radical cations and studying their reactivity patterns.[12] In the present paper, we demonstrate that several triphenylamine derivatives are capable of generating their radical cations upon reaction with Cu^{2+} in acetonitrile and that this reaction is synthetically useful for the preparation of tetraphenylbenzidine derivatives. The reaction conditions are shown in Scheme 2.

SCHEME 2. Synthesis of Tetraarylbenzidines

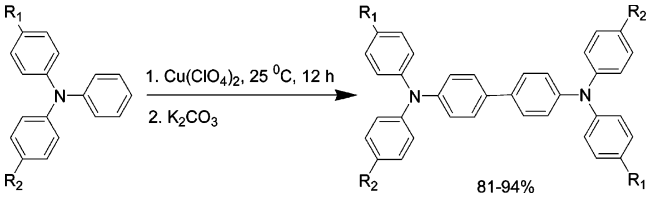

In a typical experiment, the triarylamine was mixed with $Cu(ClO_4)_2$ in acetonitrile and stirred at room temperature for 12 h. The solution turns deep blue upon addition of $Cu(ClO_4)_2$, and completion of the reaction is indicated by change of color to pale yellow. Reaction mixture was worked up as described in the experimental section to get good to excellent yields of tetraphenylbenzidines. Structures of the starting TPA and product TPB derivatives along with isolated yields are shown in Table 1.

TABLE 1. Starting Amines, Products, and Yields of Cu^{2+}-Initiated Triarylamine Dimerizations

Entry	Triarylamine	Product	Yield [%]
1		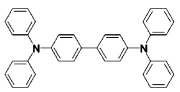	81
2	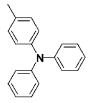	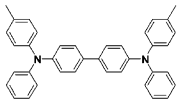	86
3	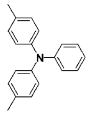	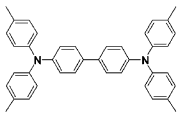	94
4	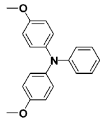	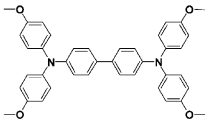	87
5	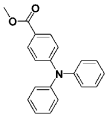	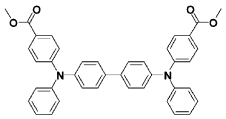	83
6	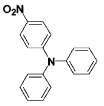	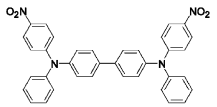	81[a]
7	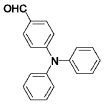	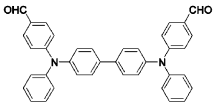	85[a]
8	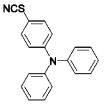	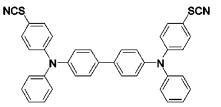	82[a]
9	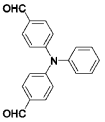	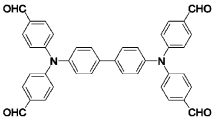	0
10	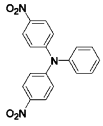	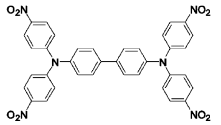	0

[a] Yields based on reacted starting material.

It can be seen from Table 1 that the reaction gives good yields even when sensitive groups such as −CHO, $-COOCH_3$, or −SCN are present in the substrate. As mentioned previously, TPB derivatives of the type shown in Table 1 are generally prepared by Ullmann reaction, which generally fails with sensitive substrates. The method presented here is obviously better than the above approaches. It may, however, be noted that electron-withdrawing substituents such as −CHO and

(9) (a) Wolfe, J. P.; Wagaw, S.; Marcoux, J.-F.; Buchwald, S. L. *Acc. Chem. Res.* **1998**, *31*, 805. (b) Hartwig, J. F. *Acc. Chem. Res.* **1998**, *31*, 852. (c) Hartwig, J. F. *Angew. Chem., Int. Ed.* **1998**, *37*, 2046.

(10) (a) Seo, E. T.; Nelson, R. F.; Fritsch, J. M.; Marcoux, L. S.; Leedy, D. W.; Adams, R. N. *J. Am. Chem. Soc*. **1966**, *88*, 3498. (b) Creason, S. C.; Wheeler, J.; Nelson, R. F. *J. Org. Chem*. **1972**, *37*, 4440. (c) Nelson, R. F.; Feldberg, S. W. *J. Phys. Chem.* **1969**, *73*, 2623.

(11) Sumalekshmy, S.; Gopidas, K. R. *Chem. Phys. Lett*. **2005**, *413*, 294.

(12) Kirchgessner. M.; Sreenath, K.; Gopidas, K. R. *J. Org. Chem*. **2006**, *71*, 9849.

$-NO_2$ exert a negative effect on this reaction. When the TPA contains one $-CHO$ or $-NO_2$ group the reactions did not go to completion. Nearly 30% of the starting materials were recovered, and the yields reported in Table 1 are based on the amount of starting materials reacted. When two $-CHO$ or $-NO_2$ groups were present, TPB formation did not take place, and most of the starting materials were recovered unchanged.

Dimerization of electrochemically generated TPA radical cation was studied in great detail and a mechanism for the dimerization was proposed previously.[10] Using cyclic voltammetry and spectroelectrochemical measurements (ESR, UV/vis/NIR), Dunsch and co-workers have clearly established the reaction pathways of several closely related, electrochemically generated triarylamine radical cations.[13] Electrochemical behaviors of several amino substituted TPA derivatives were recently studied by Chiu et al.[14] In Scheme 3 we have proposed a mechanism in line with those proposed in the electrochemical work. The first step in Scheme 3 is the formation of TPA radical cation by reaction with Cu^{2+}. Dimerization of the radical cation would lead to the dication H_2TPB^{2+}, which undergoes elimination of two protons to give TPB. The TPB generated is a better electron donor compared to TPA and hence it can donate an electron either to $TPA^{\bullet+}$ or to Cu^{2+} and generate $TPB^{\bullet+}$, which is the end product of the reaction. Steps 2 and 3 in Scheme 3 are identical to those in electrochemical dimerization. In the electrochemical reaction, oxidation of TPB to $TPB^{\bullet+}$ (step 4) occurs at the electrode, which is kept at a higher potential. In the electrochemical reaction as well as in the chemical oxidation by Cu^{2+} reported here, the end product of is $TPB^{\bullet+}$. We observed that $TPB^{\bullet+}$ can be neutralized by triethylamine (TEA) or potassium carbonate during workup to give good yields of TPB.

SCHEME 3. Mechanism Showing the Formation of $TPB^{\bullet+}$ from TPA

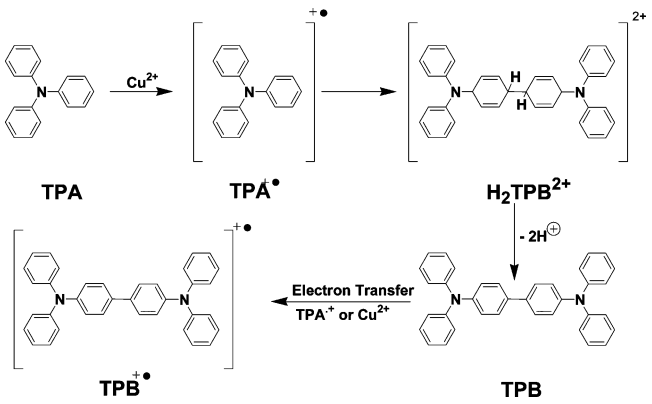

According to Scheme 3, the product TPB inhibits the reaction by reducing part of Cu^{2+} to Cu^{+} or converting part of $TPA^{\bullet+}$ back to TPA. This means that more than one equivalent of Cu^{2+} is required to drive the reaction to completion. In order to identify the optimum amount of Cu^{2+}, we have carried out the dimerization of TPA at different concentrations of Cu^{2+}. As shown in Figure 1, the product yield reached a maximum at 1.5 equiv of Cu^{2+}. Optimum concentrations of Cu^{2+} were not determined for other TPA derivatives in Table 1, and we simply used 1.5 equiv of Cu^{2+} in all these cases.

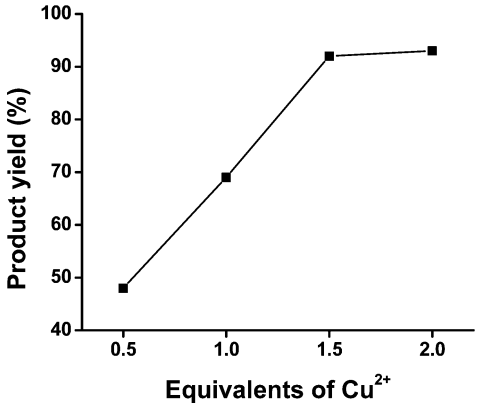

FIGURE 1. Plot of product yield vs Cu^{2+} concentration for TPA/Cu^{2+} system.

In order to clearly establish the similarity between the electrochemical and Cu^{2+} mediated dimerization reactions, we have carried out spectroscopic and kinetic investigations on the TPA/$Cu(ClO_4)_2$ system in acetonitrile. The first step is to identify if radical cations are involved in these reactions and this is best done using ESR spectroscopy. We have recorded ESR spectra of all the TPA derivatives listed in Table 1 in the presence of Cu^{2+}. All TPA derivatives which gave benzidines as products in this reaction exhibited ESR signals, and some examples are given in Figure 2 (see the Supporting Information (SI) for remaining ESR spectra).

The paramgnetic Cu^{2+} shows a ESR signal around 3000 G. When 1 equiv of a TPA derivative was added, the ESR signal at 3000 G completely disappeared and new signals corresponding to radical cations of the TPA appeared immediately near 3250 G. This clearly indicates that radical cations of the TPAs are formed as a result of electron transfer from the amine to the paramagnetic Cu^{2+}. The ESR signals decayed with time and the spectra presented in Figure 2 were collected during the first 3 min of mixing. In all cases, we got almost identical single line ESR spectra. Stamires and Turkevich have previously observed unresolved single line ESR spectrum for $TPA^{\bullet+}$ at relatively high concentrations.[15] The lack of hyperfine structure was attributed to interactions of the radical cations with each other. In the case of the diformyl and dinitro derivatives (entries 9 and 10 in Table 1), ESR spectra corresponding to amine radical cations were not observed and the signal due to Cu^{2+} did not disappear.

We have monitored the dimerization reaction using absorption spectroscopy. TPA do not absorb above 370 nm in acetonitrile solution. Upon addition of 1.5 equiv of $Cu(ClO_4)_2$, an intense absorption band in the 600−800 nm region is formed and as a result the solution turned blue. Absorption spectrum of TPA/Cu^{2+} system in acetonitrile immediately after mixing is shown in Figure 3a (λ_{max} = 680 nm). Lewis and Lipkin had generated $TPA^{\bullet+}$ by photoionization of TPA in rigid matrix at low temperature.[16] $TPA^{\bullet+}$ thus generated exhibited absorption maximum at 660 nm. Hasegawa had shown that $TPA^{\bullet+}$ generated by the chemical oxidation of TPA with acid zeolites absorbed at 678 nm.[17] Hall obtained $TPA^{\bullet+}$ by reacting TPA with silica−alumina catalyst and reported its absorption maxi-

(13) (a) Rapta, P.; Rohde, D.; Hartmann, H.; Dunsch, L. *Tetrahedron Lett.* **2006**, *47*, 7587. (b) Rapta, P.; Zeika, O.; Rohde, D.; Hartmann, H.; Dunsch, L. *ChemPhysChem* **2006**, *7*, 863.

(14) Chiu, K. Y.; Su, T. X.; Li, J. H.; Lin, T.-H.; Liou, G.-S.; Cheng, S.-H. *J. Electroanal. Chem.* **2005**, *575*, 95.

(15) Stamires, D. N.; Turkevich, J. *J. Am. Chem. Soc.* **1963**, *85*, 2557.

(16) Lewis, G. N.; Lipkin, E. *J. Am. Chem. Soc.* **1942**, *64*, 2801.

(17) Hasegawa, H. *J. Phys. Chem.* **1962**, *66*, 834.

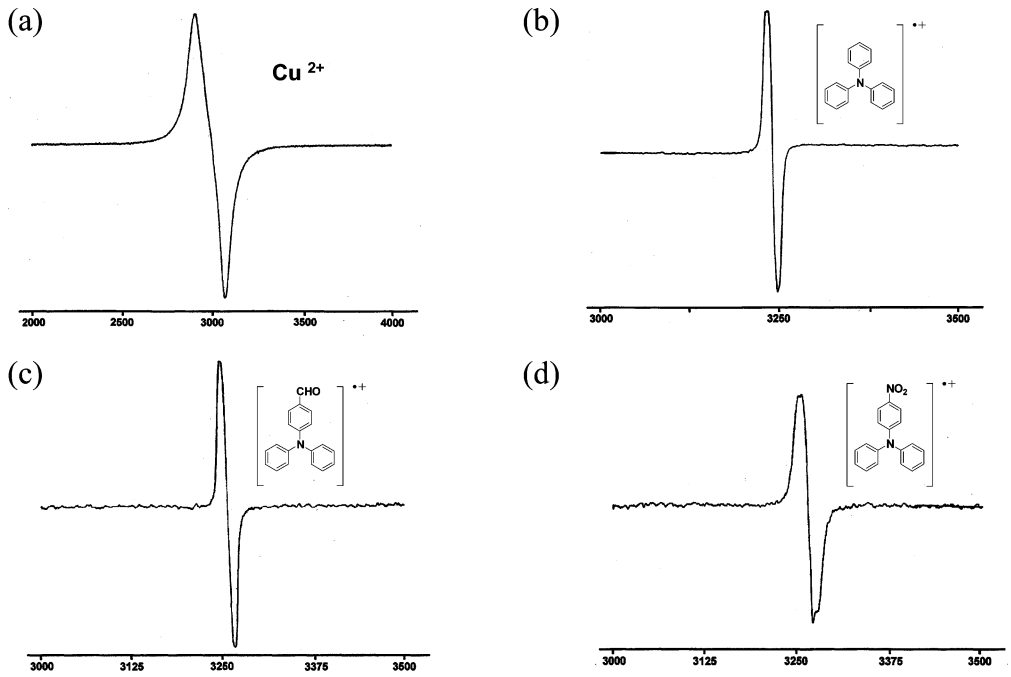

FIGURE 2. (a) ESR spectrum of 0.1 M solution of $Cu(ClO_4)_2$ in ACN; (b−d) ESR spectra of 1 mmol of triarylamine with 1 mmol of $Cu(ClO_4)_2$ in ACN.

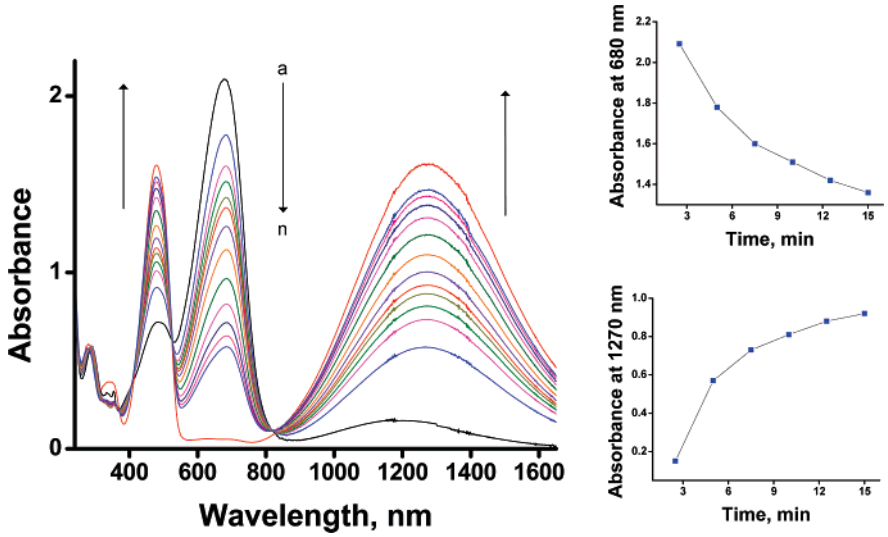

FIGURE 3. Time-dependent changes in the absorption spectrum of a solution containing TPA (1×10^{-4} M) and $Cu(ClO_4)_2$ (1.5×10^{-4} M) in ACN. Spectrum "n" was taken after 24 h. Insets show the time dependences of absorptions at 680 and 1270 nm.

mum as 660 nm.[18] Dollish and Hall generated $TPA^{\bullet+}$ by reacting TPA with iodine and showed that this species absorbs around 660 nm.[19] Based on these reports and our own previous findings,[10,11] we assign the 680 nm band in Figure 2a to $TPA^{\bullet+}$.

The absorption due to $TPA^{\bullet+}$ was monitored as a function of time and this is shown in Figure 3b−n. It can be seen that the absorption due to $TPA^{\bullet+}$ decreased with time along with concomitant increase in the absorptions in the 400−580 nm and 900−1600 nm regions. Presence of the isosbestic points in Figure 3 suggest that the species responsible for the new absorptions originate from $TPA^{\bullet+}$. This is also clear from the decay at 680 nm and the matching growth at 1270 nm, shown as insets in Figure 2. The final spectrum (Figure 3n) was very stable (more than 24 h) and is assigned to $TPB^{\bullet+}$ based on literature reports and our own results.[10,11,15−20] For example, Seo et al. observed that electrolysis of TPA or TPB solutions at +1.15 V gave the same species having absorption at 480 nm, and this was identified as $TPB^{\bullet+}$.[10a] Dollish and Hall[19] generated $TPA^{\bullet+}$ by oxidizing TPA with silica−alumina catalyst and observed that the initial absorption band at 660 nm assignable to $TPA^{\bullet+}$ decreased with time leading to the formation a new band at 480 nm. This band was assigned to $TPB^{\bullet+}$, arising from a $\pi-\pi^*$ transition. Recent studies have also established the existence of a long wavelength band in the

(18) Hall, W. K. *J. Catalysis* **1962**, *1*, 53.
(19) Dollish, F. R.; Hall, W. K. *J. Phys. Chem.* **1965**, *69*, 2127.
(20) Rapta, P.; Fáber, R.; Dunsch, L.; Neudeck, A.; Nuyken, O. *Spectrochim. Acta* **2000**, *56 A*, 357.

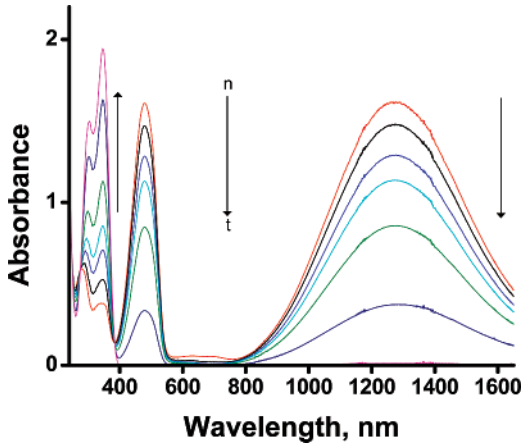

FIGURE 4. Effect of addition of increasing amounts of TEA to solution of spectrum "n" in Figure 3.

1000−1600 nm region for $TPB^{\bullet+}$, which is assigned to the intervalence charge-transfer excitation.[21] $TPB^{\bullet+}$ consists of a neutral TPA unit and a $TPA^{\bullet+}$ unit. The intervalence charge-transfer band arises as a result of photoexcited electron transfer from the neutral TPA moiety to the $TPA^{\bullet+}$. These reports are in agreement with the assignments made here. We observed that $TPB^{\bullet+}$ could also be generated by the reaction of Cu^{2+} with TPB and the spectrum obtained was identical to Figure 3n, which further confirms the assignment.

The absorptions due to $TPB^{\bullet+}$ at 400−580 nm and at 900−1600 nm were very stable for several hours. Upon addition of excess TEA these bands disappeared leading to the formation of a new absorption below 400 nm (Figure 4). Based on a comparison with authentic sample, the new band was assigned to TPB. We observed that $TPB^{\bullet+}$ can also be quenched by aqueous K_2CO_3, although the mechanism of quenching is not very clear. Thus, K_2CO_3 was employed in the workup procedure.

Although we have proposed a few intermediates for the reaction in Scheme 3, the spectroscopic studies (Figures 2 and 3) could identify only $TPA^{\bullet+}$ and $TPB^{\bullet+}$. The isosbestic points in Figure 3 suggest that $TPA^{\bullet+}$ is converted smoothly into $TPB^{\bullet+}$, and there are no observable intermediates in this transformation. Formation of $TPB^{\bullet+}$ from $TPA^{\bullet+}$, however, has to involve dimerization of the radical cation (radical−radical coupling) to the dicationic species H_2TPB^{2+}, deprotonation of H_2TPB^{2+} to TPB and oxidation of TPB to $TPB^{\bullet+}$ as shown in Scheme 3. Most probably, H_2TPM^{2+} and TPB are not observed in Figure 3 because the deprotonation and electron-transfer reactions are very fast compared to the dimerization reaction. In general, radical cations and dications are highly acidic compared to neutral molecules, and hence deprotonation of H_2-TPB^{2+} to neutral TPB molecule is expected to be very fast. The TPB thus formed is a better electron donor (E_{ox} = 0.69V vs SCE) than TPA (E_{ox} = 0.92 V vs SCE). Hence, a spontaneous electron exchange reaction between the two can take place, leading to the formation of $TPB^{\bullet+}$.[10a] If Cu^{2+} is present in excess, electron transfer from TPB to Cu^{2+} can also occur spontaneously, leading to the formation of $TPB^{\bullet+}$.

(21) (a) Lambert, C.; Nöll, G. *J. Am. Chem. Soc.* **1999**, *121*, 8434. (b) Nelsen, S. F. *Chem. Eur. J.* **2000**, *6*, 581. (c) Lambert, C.; Noll, G. *J. Chem. Soc., Perkin Trans. 2* **2002**, 2039. (d) Littleford, R. E.; Paterson, M. A. J.; Low, P. J.; Tackley, D. R.; Jayes, L.; Dent, G.; Cherryman, J. C.; Brown, B.; Smith, W. E. *Phys. Chem. Chem. Phys.* **2004**, *6*, 3257. (e) Low, P. J.; Paterson, M. A. J.; Puschmann, H.; Goeta, A. E.; Howard, J. A. K.; Lambert, C.; Cherrymann, J. C.; Tackley, D. R.; Leeming, S.; Brown, B. *Chem. Eur. J.* **2004**, *10*, 83.

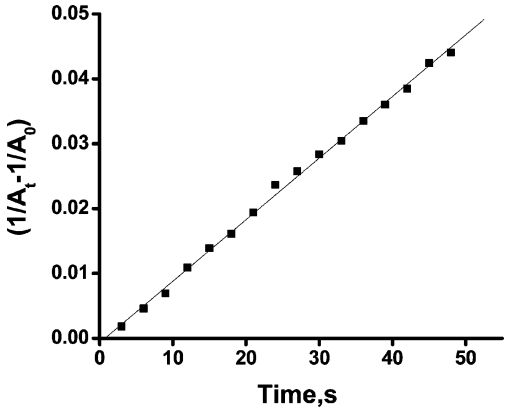

FIGURE 5. Plot of $1/A_t - 1/A_0$ vs time for TPA/Cu^{2+} system.

The mechanism presented in Scheme 3 is based on the reports dealing with the electrochemical oxidations of triphenylamine. In electrochemical reactions, high concentrations of the radical species are generated at the electrodes and radical−radical coupling is the preferred pathway.[10b] In the present case, where the reaction occurs in bulk solution another mechanism involving addition of $TPA^{\bullet+}$ to TPA (radical-parent coupling) also needs to be considered. The coupled product can undergo electron transfer with Cu^{2+} to generate H_2TPB^{2+}. A distinction between the two reaction pathways could be made using kinetic experiments. The radical−radical coupling is second order with respect to $TPA^{\bullet+}$ whereas the radical-parent pathway is first-order each in $TPA^{\bullet+}$ and TPA. The absorption due to $TPA^{\bullet+}$ occurs in a region where TPA or other intermediates in Scheme 3 do not interfere. This gives us an opportunity to determine the order of the reaction by monitoring the absorption due to $TPA^{\bullet+}$. The time dependence of the absorbance due to $TPA^{\bullet+}$ at 680 nm plotted as per second-order kinetics is shown in Figure 5. The straight line is a fit to second-order kinetics. Good match of the data to the fit strongly supported the radical−radical coupling mechanism shown in Scheme 3. The rate constant obtained for the dimerization of TPA was 9.3×10^{-4} M^{-1} s^{-1}. The value obtained is several orders smaller than that reported by Creason et al.[10b] ($k = 1.2 \times 10^3$ M^{-1} s^{-1}) for the electrochemical dimerization. The large value in the electrochemical work is due to the large concentration of the ion radicals at the electrode surface. It is to be mentioned here that the kinetic experiments were carried out only in the case of TPA. For other derivatives shown in Table 1, particularly those with electron-withdrawing substituents, reaction of the amines with Cu^{2+} was slow. Thus, formation of radical cations interfered with its decay and determination of dimerization rate constants required prior knowledge about the rate of formation of the amine radical cations. Stopped-flow experiments to determine these rates are being planned.

An examination of Table 1 shows that the dimerization reaction is slow or incomplete when the TPAs contain electron-withdrawing groups. In the case of the dinitro derivative, the radical cation was not formed and the reaction did not proceed at all. These factors can be attributed to the free energy changes associated with the radical cation formation. Free energy change for the electron-transfer reaction (1) can be calculated using the standard expression

$$\Delta G^\circ = E_{ox} - E_{red} - e^2/d\epsilon \qquad (2)$$

TABLE 2. E_{ox} for TPA Derivatives and ΔG^0 Associated with Radical Cation Formation

triarylamine[a]	E_{ox} vs SCE	ΔG^0
$R_1 = H, R_2 = H$	0.92	−0.210
$R_1 = H, R_2 = CH_3$	0.90	−0.230
$R_1 = CH_3, R_2 = CH_3$	0.88	−0.250
$R_1 = OCH_3, R_2 = OCH_3$	0.76	−0.370
$R_1 = H, R_2 = SCN$	1.02	−0.101
$R_1 = H, R_2 = COOCH_3$	1.05	−0.080
$R_1 = H, R_2 = CHO$	1.08	−0.050
$R_1 = H, R_2 = NO_2$	1.16	+0.030
$R_1 = CHO, R_2 = CHO$	1.21	+0.080
$R_1 = NO_2, R_2 = NO_2$	1.35	+0.220

[a] R_1 and R_2 as in Scheme 2.

where E_{ox} is the oxidation potential of the TPA derivatives, E_{red} is the reduction potential of Cu^{2+}, d is the center-to-center distance between TPA and $Cu(ClO_4)_2$ hexahydrate in the collision complex, and ϵ is the dielectric constant (= 37) of ACN. E_{ox} values for all the TPA derivatives were measured using cyclic voltammetry and these are given in Table 2. E_{red} of Cu^{2+} in ACN is + 0.952 V vs SCE. In fact, this value is approximately 1 V more positive than E_{red} in water, and the gain in energy by changing the solvent to ACN is attributed to formation of the stable tetrakis(acetonitrile)copper(I) complex immediately following the reduction of Cu^{2+} to Cu^+.[22] Reaction (1) takes place only in acetonitrile, and part of the driving force for the reaction comes form the free energy of formation of $[Cu(CH_3CN)_4]^+$ complex. Hence, reaction (1) should be modified as shown in (3).

$$\text{amine} + Cu^{2+} \xrightarrow{CH_3CN} \text{amine}^{\bullet+} + [Cu(CH_3CN)_4]^+ \quad (3)$$

Under these conditions, it is advisable to replace E_{red} in eq 2 with the reduction peak potential (E_p) obtained by linear sweep voltammetry. For the reduction of Cu^{2+} in ACN, we obtained E_p as +1.082. The Coulombic term in eq 2 was calculated assuming $d = 8$ Å. Using these values, the $\Delta G°$ associated with the radical cation formation was calculated for all TPA derivatives shown in Table 1 and the values are presented in Table 2.

Analysis of Tables 1 and 2 showed that there is good correlation between the $\Delta G°$ values and product yields. For the first six entries in Table 2, $\Delta G°$ values are negative and yields of TPB are very good. For the mononitro derivative (entry 7), the $\Delta G°$ value is slightly positive and the reaction did not go to completion. In the case of diformyl and dinitro derivatives, TPB derivatives were not formed because the $\Delta G°$ for formation of radical cations were positive. This shows that a correlation exists between $\Delta G°$ of radical cation fromation and yields of TPB in the systems studied.

Conclusion

In summary, we have shown that the reaction of triphenylamine derivatives with Cu^{2+} in ACN generates radical cations of the amines and that this reaction can be exploited for the synthesis of tetraphenylbenzidine derivatives. A mechanism for the formation of TPB derivatives is also proposed. The mechanism is confirmed by spectroscopic and kinetic studies. Finally, the yields of the TPB derivatives are correlated to the free energy change associated with the formation of radical cations.

Experimental Section

1. General Methods. Absorption spectra were recorded on a UV−vis−NIR spectrophotometer. The ^1H and ^{13}C NMR spectra were recorded in $CDCl_3$ on a FT-NMR (300 MHz) spectrometer, and the chemical shifts, δ, are referred to TMS. The FAB mass spectra were recorded on a spectrometer. Redox potentials of Cu(II) and all the TPA derivatives were measured using a cyclic voltammetric analyzer, with a conventional three-electrode system. The ESR spectra were recorded using an ESR spectrometer operating at X-band frequencies and having a 100 kHz field modulation. $Cu(ClO_4)_2$ and triphenylamine were commercial samples. Other triphenylamine derivatives were prepared by the reactions of primary or secondary amines with aryl halides as per reported procedures.[8] All experiments were carried out at room temperature (25 ± 1 °C), unless otherwise mentioned.

2. General Procedure for Preparation of Tetraphenylbenzidines. A solution of $Cu(ClO_4)_2$ hexahydrate (222 mg, 0.60 mmol) in ACN (10 mL) was added to a solution of the triarylamine (0.4 mmol) in ACN (20 mL) at room temperature, and the mixture was stirred for 12 h. Solid K_2CO_3 (500 mg) and water (1 mL) were added, and stirring was continued for 0.5 h. Filtered and the solids were washed twice with chloroform. The combined organic extracts were filtered through a short pad of alumina. The solvent was removed and the residue so obtained was recrystallized form dichloromethane-hexane mixture to give pure products. Yields shown in Table 1 are those of pure products. For entries 6−8 in Table 1, the organic residues were chromatographed over neutral alumina. Elusion with a mixture of chloroform−hexane (1:9) gave the unreacted starting materials. Further elution with chloroform−hexane (1:4) gave the pure products.

***N,N,N′,N′*-Tetraphenylbiphenyl-4,4′-diamine(1):**[8c] yield 81%; ^1H NMR ($CDCl_3$) δ 6.99−7.45 (m, 28H); ^{13}C NMR ($CDCl_3$) δ 122.76, 124.04, 124.24, 127.25, 129.21, 134.66, 146.66, 147.65; MS (FAB) *m*/*z* 488 (M^+). Anal. Calcd for $C_{36}H_{28}N_2$: C, 88.49; H, 5.78; N, 5.73. Found: C, 88.02; H, 6.21; N, 5.87.

***N,N′*-Diphenyl-*N,N′*-di(*p*-tolyl)biphenyl-4,4′-diamine(2):**[8f] yield 86%; ^1H NMR ($CDCl_3$) δ 2.32 (s, 6H), 7.07−7.42 (m, 26H); ^{13}C NMR ($CDCl_3$) δ 20.82, 122.33, 123.52, 123.72, 125.00, 127.15, 129.12, 129.93, 132.83, 134.36, 145.11, 146.82, 147.87; MS (FAB) *m*/*z* 516 (M^+). Anal. Calcd for $C_{38}H_{32}N_2$: C, 88.34; H, 6.24; N, 5.42. Found: C, 88.08; H, 6.50; N, 5.32.

***N,N,N′,N′*-Tetra(*p*-tolyl)biphenyl-4,4′-diamine(3):**[8d] yield 94%; ^1H NMR ($CDCl_3$) δ 2.15 (s, 12H), 6.83−6.94 (m, 20H), 7.25 (d, 4H); ^{13}C NMR ($CDCl_3$) δ 21.01, 123.15, 124.68, 127.24, 130.05, 132.48, 134.15, 145.51, 147.17; MS (FAB) *m*/*z* 544 (M^+). Anal. Calcd for $C_{40}H_{36}N_2$: C, 88.20; H, 6.66; N, 5.14. Found: C, 87.81; H, 7.16; N, 5.45.

***N,N,N′,N′*-Tetrakis(4-methoxyphenyl)biphenyl-4,4′-diamine (4):**[21a] yield 87%; ^1H NMR ($CDCl_3$) δ 3.78 (s, 12H), 6.81 (d, 8H), 6.96 (m, 4H), 7.05 (d, 8H), 7.34 (d, 4 H); ^{13}C NMR ($CDCl_3$) δ 55.45, 114.62, 121.08, 126.37, 126.84, 132.99, 140.92, 147.35, 155.67; MS (FAB) *m*/*z* 608 (M^+). Anal. Calcd for $C_{40}H_{36}N_2O_4$: C, 78.92; H, 5.96; N, 4.60. Found: C, 78.86; H, 6.45; N, 4.64.

***N,N′*-Bis(*p*-carbomethoxyphenyl)-*N,N′*-di(phenyl)biphenyl-4,4′-diamine (5):** yield 83%; ^1H NMR ($CDCl_3$) δ 3.88 (s, 6H), 7.03 (d, 4H), 7.14−7.19 (m, 10H), 7.30−7.35 (m, 4H), 7.50 (d, 4H), 7.86 (d, 4H); ^{13}C NMR ($CDCl_3$) δ 52.71, 119.34, 121.39, 122.35, 124.81, 126.71, 128.75, 130.71, 131.94, 136.24, 146.54, 145.77, 151.77, 166.86; MS (FAB) *m*/*z* 605 (M + 1). Anal. Calcd for $C_{40}H_{32}N_2O_4$: C, 79.45; H, 5.33; N, 4.63. Found: C, 79.01; H, 5.75; N, 4.90.

***N,N′*-Bis(4-nitrophenyl)-*N,N′*-diphenylbiphenyl-4,4′-diamine-(6).** 30% starting amine was recovered: yield based on reacted SM

(22) (a) Parker, A. J. *Pure Appl. Chem.* **1981**, *53*, 1437. (b) Persson, I. *Pure Appl. Chem.* **1986**, *58*, 1153. (c) Cox, B. G.; Jedral, W.; Palou, J. *J. Chem. Soc. Dalton Trans.* **1988**, 733. (d) Kamau, P.; Jordan, R. B. *Inorg. Chem.* **2001**, *40*, 3879.

81%; ^{1}H NMR ($CDCl_3$) δ 6.90 (d, 4H), 7.12−7.17 (m, 10H), 7.28−7.33 (m, 4H), 7.48 (d, 4H), 7.97 (d, 4H); ^{13}C NMR ($CDCl_3$) δ 118.57, 125.45, 125.86, 126.41, 126.55, 128.16, 129.98, 137.10, 140.35, 144.98, 145.50, 153.23; MS (FAB) *m*/*z* 578 (M^+). Anal. Calcd for $C_{36}H_{26}N_2O_4$: C, 74.73; H, 4.53; N, 9.68. Found: C, 74.31; H, 5.03; N, 9.51.

***N*,*N*′-Bis(*p*-formylphenyl)-*N*,*N*′-diphenylbiphenyl-4,4′-diamine (7).** 20% starting amine was recovered: yield based on reacted SM 85%; ^{1}H NMR ($CDCl_3$) δ 7.07 (d, 4H), 7.16−7.25 (m,10H), 7.33−7.38 (m, 4H), 7.53 (d, 4H), 7.69 (d, 4H), 9.81(s, 2H); ^{13}C NMR ($CDCl_3$) δ 119.75, 125.23, 126.16, 126.34, 127.92, 129.34, 129.77, 131.29, 136.62, 145.39, 146.02, 153.11, 190.38; MS (FAB) *m*/*z* 545 (M + 1). Anal. Calcd for $C_{38}H_{28}N_2O_2$: C, 83.80; H, 5.18; N, 5.14. Found: C, 83.43; H, 5.61; N, 5.34.

***N*,*N*′-Diphenyl-*N*,*N*′-bis(4-thiocyanatophenyl)biphenyl-4,4′-diamine (8).** 10% starting amine was recovered: yield based on reacted SM 82%; ^{1}H NMR ($CDCl_3$) δ 7.01 (d, 4H), 7.08 (d, 10H), 7.23−7.33 (m, 8H), 7.42 (d, 4H); ^{13}C NMR ($CDCl_3$) δ 113.73, 121.96, 122.91, 123.41, 125.50, 126.71, 128.64, 130.63, 134.02, 135.90, 145.67, 146.39, 149.65; MS (FAB) *m*/*z* 602 (M^+). Anal. Calcd for $C_{38}H_{26}N_4S_2$: C, 75.72; H, 4.35; N, 9.29. Found: C, 75.49; H, 4.80; N, 9.14.

Acknowledgment. We thank the Council of Scientific and Industrial Research (CSIR) and Department of Science and Technology (DST), Government of India, for financial support. K.S. and C.V.S. thank CSIR and V.K.R.K. thanks UGC for their Research Fellowships. We thank Professor P. Sambasiva Rao and Dr. B. Natarajan of the Department of Chemistry, University of Pondicherry, for the ESR spectra. This is contribution number NIIST-PPG-261.

Supporting Information Available: ^{1}H NMR and ^{13}C NMR spectra for all compounds and ESR spectra. This material is available free of charge via the Internet at http://pubs.acs.org.

JO800349N